PCCP

ROYAL SOCIETY OF CHEMISTRY

COMMUNICATION

View Article Online
View Journal | View Issue

Cite this: *Phys. Chem. Chem. Phys.*, 2026, **28**, 1089

Received 14th October 2025,
Accepted 11th December 2025

DOI: 10.1039/d5cp03956h

rsc.li/pccp

Smartphone light-driven electrocatalytic polymerization of thiophenes†

Gerardo Salinas, *[a] Rana Nakar,[b] Getnet Kassahun,[c] Jochen Lang,[d] Matthieu Raoux,[d] Damien Thuau,[c] Mamatimin Abbas,[c] Eric Cloutet[b] and Alexander Kuhn *[a]

Herein, we take advantage of the photoelectric effect produced on light-emitting diodes to induce a kinetically controlled electrocatalytic polymerization of 3,4-alkoxythiophenes. Wireless polymerization was achieved by fine-tuning the irradiation time, the power density and the molecular structure of the thiophenes. A smartphone based light-driven system is introduced as a simple and low cost polymerization approach to π-conjugated films.

Organic electroactive materials have gained considerable attention in multiple applications, ranging from energy conversion to sensing.[1] Among all these materials, π-conjugated polymers stand out due to their rather fast charging/discharging transition, good optical properties and efficient conductivity.[2] Commonly, these materials are synthesized *via* an oxidative radical polymerization mechanism,[3] which is triggered chemically by using homogeneous catalysts (strong oxidizing agents)[4] or electrochemically by controlling the applied potential or current.[5] Due to the possible fine-tuning of the thermodynamic or kinetic parameters of the polymerization, electrochemical methods allow efficient control of the morphology and optoelectronic properties of the films.[6] Nonetheless, this methodology requires a direct connection of the electrode to a potentiostat, limiting its use for *in situ* applications, thus the development of wireless strategies is highly desired.

Recently, bipolar electrochemistry (BE) has emerged as a powerful approach to achieve wireless electropolymerization.[7] It is based on the induction of a polarization potential difference (ΔV) across a conducting object acting as a bipolar electrode (BPE), due to the presence of an electric field in solution. When ΔV overcomes the threshold polarization potential difference (ΔV_{min}) associated with the oxidation and reduction of the monomer and a sacrificial redox probe, respectively, electropolymerization takes place at the anodic extremity of the BPE. This approach has been extensively used for the synthesis of films and fibers of poly(3,4-ethylenedioxythiophene) (PEDOT).[7] Although interesting, BE often requires a high-voltage power source in order to produce the appropriate electric field.

An interesting alternative is to take advantage of the voltage-generating function of light-emitting diodes (LEDs). In recent years, these microelectronic devices have gained considerable attention as optical transducers of chemical information.[8] However, due to the n- and p-type semiconductors composing the diodes, LEDs can not only produce light, but also generate a significant difference of voltage when irradiated with photons with appropriate wavelength (ΔV_{hv}).[9] This photoelectric effect has been exploited in sensing, electrochemiluminescence devices and water electrolysis.[9] In this work, we take advantage of the light-induced ΔV_{hv} to power the electrocatalytic polymerization of different 3,4-alkoxy thiophenes. By irradiating a red LED with white light, a sufficient ΔV_{hv} is induced to trigger the oxidation and reduction of the monomer and of a sacrificial redox probe, respectively. Furthermore, by fine-tuning the chemical structure of the thiophene unit, it is possible to decrease the ΔV_{min} required to trigger the redox reactions. Moreover, this approach allows producing π-conjugated films with well-defined redox signals, even when irradiating with the light of a mobile phone. This straightforward method enables the wireless synthesis of π-conjugated polymers with a simple low-cost experimental setup.

As stated above, the light-driven electrocatalytic polymerization takes advantage of the ΔV_{hv} induced across an LED when irradiated with photons of appropriate wavelength. In a first order approximation, this ΔV_{hv} can trigger redox reactions at each extremity of the diode, as long as it overcomes the ΔV_{min} associated with the electroactive species in solution. In the present case, the oxidation of two different 3,4-alkoxythiophenes, *i.e.* EDOT and 3,4-propylenedioxythiophene (ProDOT) (Fig. 1a), and the reduction of benzoquinone (Q) were used as model reactions.

[a] *University of Bordeaux, CNRS, Bordeaux INP, ISM UMR 5255, 33600, Pessac, France. E-mail: kuhn@enscbp.fr, gerardo.salinassanchez@enscbp.fr*
[b] *University of Bordeaux, CNRS, Bordeaux INP, LCPO, UMR 5629, 33615 Pessac, France*
[c] *University of Bordeaux, CNRS, Bordeaux INP, IMS, UMR 5218, 33400, Talence, France*
[d] *University of Bordeaux, CNRS, Bordeaux INP, CBMN, UMR 5248, 33600 Pessac, France*

† Dedicated to Prof. Jumras Limtrakul, VISTEC, on the occasion of his 72nd birthday, for his important contributions to the field of catalysis.

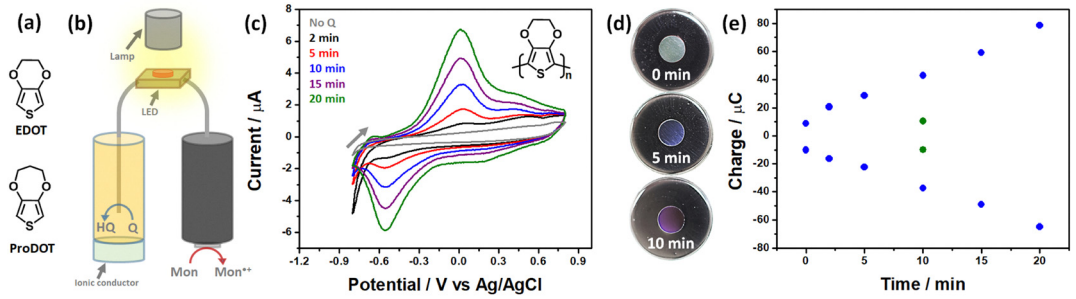

Fig. 1 (a) Chemical structures of EDOT and ProDOT. (b) Schematic illustration of the experimental setup and the principle of the light-driven electrocatalytic polymerization. (c) Potentiodynamic characterization of PEDOT films deposited on Pt electrodes under constant P_{hv} (3.7 kW cm^{-2}) as a function of t_{hv} (indicated in the figure), obtained in a monomer-free 0.1 M tetrabutylammonium perchlorate/acetonitrile (TBAP/ACN) solution, v = 50 mV s^{-1}. The grey curve represents the potentiodynamic response in the absence of quinone. (d) Optical pictures of the electrode surfaces modified for different t_{hv} (indicated in the figure) by the electropolymerization of EDOT. (e) Q_a and Q_c variation as a function of t_{hv} obtained during the light-assisted electrocatalytic polymerization of EDOT. The green dots represent Q_a and Q_c obtained in the absence of quinone.

First, the individual potentiodynamic characterization of EDOT and ProDOT (10 mM), and Q (10 mM) was performed in a 0.1 M tetrabutylammonium perchlorate (TBAP)/acetonitrile (ACN) solution. During the anodic sweep, EDOT and ProDOT present a characteristic oxidation peak with an onset potential around 1.1 V *vs.* Ag/AgCl and 1.2 V *vs.* Ag/AgCl, respectively, whereas in the cathodic direction, the reduction of Q occurs at −0.4 V *vs.* Ag/AgCl (Fig. S1). Thus, ΔV_{min} values of ≈1.5 V and ≈1.6 V are required to trigger the anodic electropolymerization of the monomers *via* the voltage-generating function of a diode. In order to corroborate this, the ΔV_{hv} induced by a red LED was evaluated as a function of power density (P_{hv}). The photo-induced ΔV_{hv} was monitored by connecting a voltammeter to the terminals of the diode. A tungsten–halogen light source coupled to a fiber-bundle was used to irradiate the diode. As shown in Fig. S2 (black line), at low P_{hv} values (below 2×10^{-3} kW cm^{-2}), the induced ΔV_{hv} remains below 0.3 V. However, when P_{hv} is increased gradually, ΔV_{hv} increases up to 1.6 V, which is the minimum required to trigger the corresponding redox reactions.

After this set of experiments, we evaluated the possible light-driven electrocatalytic polymerization of EDOT and ProDOT. A Pt wire and a Pt disk electrode were dipped into two chambers separated by a glass frit, filled with a 0.1 M TBAP/ACN solution containing either Q (10 mM) or a monomer (10 mM), and then connected to the cathode and anode of a red-LED, respectively (Fig. 1b and Fig. S3). It is important to highlight that under these experimental conditions, additional interfacial resistances will impact the polarization potential, leading to a 100 mV decrease in driving force (Fig. S2 red line). Nonetheless, by irradiating with a P_{hv} of 3.7 kW cm^{-2}, it is possible to produce a sufficient ΔV_{hv} to trigger the redox reactions, and the amount of deposited PEDOT was evaluated as a function of irradiation time (t_{hv}). For this, the potentiodynamic response of the films after polymerization was recorded in a monomer-free 0.1 M TBAP/ACN solution. As expected, the irreversible charge/discharge signals (ΔE_p ≈ 560 mV), characteristic of PEDOT, appeared gradually when increasing t_{hv} (Fig. 1c). Furthermore, the discharged polymer presents a slightly blue color that progressively changes to dark purple as t_{hv} increases (Fig. 1d). Moreover, the plot of the anodic (Q_a) and cathodic (Q_c) charge as a function of t_{hv} presents a rather linear correlation (Fig. 1e blue dots). Such a linearity is characteristic of kinetically controlled electropolymerization, thus, under these conditions, the oxidative dimerization pathway occurs at a rather slow rate.[3a] This leads to an ordered monomer–oligomer coupling, which in turn favours the formation of long-chain oligomers, as evidenced by the well-defined redox peaks between 0.2 V *vs.* Ag/AgCl and −0.75 V *vs.* Ag/AgCl (Fig. 1c). The general validity of the approach was verified by performing the light-driven electropolymerization of ProDOT. For a constant P_{hv} value (3.7 kW cm^{-2}), the characteristic irreversible redox signals of poly-ProDOT (PProDOT, ΔE_p ≈ 600 mV) appeared gradually as a function of t_{hv} (Fig. S4a), producing a brownish coloured film (inset of Fig. S3b). Once again, a linear correlation between Q_a and Q_c and t_{hv} was obtained, corroborating the kinetically controlled electropolymerization (Fig. S4b blue dots). The electrocatalyzed polymerization of ProDOT is rather surprising, since a ΔV above 1.6 V is required to trigger the redox reactions. However, it is possible to assume that under these conditions, the diode generates a sufficient ΔV_{hv}, triggering the oxidation of the monomer. Thus, once a few charged short-chain oligomers of PProDOT are formed, they self-catalyse the oligomerization *via* solid-state redox processes.[10] To verify the contribution of the sacrificial redox probe on the electropolymerization kinetics, a control experiment was carried out in the absence of quinone under constant P_{hv} and t_{hv} (3.7 kW cm^{-2} and 10 min, respectively). As expected, under these conditions, only the characteristic response associated with the capacitive current of the electrode/solution interface was obtained (Fig. 1c and Fig. S4a, grey line). Furthermore, the recorded Q_a and Q_c values are found to be comparable to the ones obtained in the absence of light (Fig. 1e and Fig. S4b, green dots).

After this set of experiments, demonstrating the light-driven electropolymerization, we evaluated the influence of the magnitude of P_{hv} on the synthesis of π-conjugated polymers. In this case, the electrolysis was carried out with a constant t_{hv} (10 min) in a 10 mM EDOT, 0.1 M TBAP/ACN solution. At low P_{hv} values (below 1.5 kW cm^{-2}), the potentiodynamic analysis of the modified electrode in a monomer-free solution exhibits only the capacitive response of the electrode/solution interface

(Fig. S5). Above this value, the polymerization begins, as evidenced by the low intensity redox signals of PEDOT. From this point onwards, the charging/discharging response of the film increases (Fig. S5). This provides evidence that the electropolymerization takes place only when the induced ΔV_{hv} exceeds the ΔV_{min} associated with the oxidation and reduction of EDOT and quinone, respectively (above 1.5 V). In order to overcome this thermodynamic limitation, we decided to fine-tune the chemical structure of 3,4-alkoxythiophenes. It is well-established that the oxidation potential of π-conjugated groups decreases with an increase in the conjugation length, meaning that the oxidation potential of the monomer is higher than those of the dimer and the trimer.[3a] In particular, π-conjugated trimeric units have gained considerable attention due to their low oxidation potential and easy synthesis.[11] Thus, two different 3,4-alkoxythiophene trimers were synthesized, bis[3,4-ethylenedioxythiophene]-2-hexyl-EDOT (C_6-Tri-EDOT) and bis[3,4-ethylenedioxythiophene]-3,4-(2,2-dimethylpropylenedioxy)thiophene (C_2-EPE) (Fig. 2a). Both target trimers were synthesized following a three-step procedure; (i) formation of the EDOT/ProDOT derivatives, (ii) an α-,α-dibromination, and finally (iii) a Suzuki coupling with EDOT boronic ester (Schemes S1 and S2). All intermediates and final products were characterized by ^{1}H and ^{13}C nuclear magnetic resonance (NMR) spectroscopy, and the trimeric structures were further confirmed by high resolution mass spectroscopy (HRMS). Detailed synthetic procedures and characterization data are provided in the SI (Fig. S6–S17).

The oxidation of C_6-Tri-EDOT and C_2-EPE presents a peak between 0.45 V *vs.* Ag/AgCl and 0.5 V *vs.* Ag/AgCl, with a threshold potential of 0.3 V *vs.* Ag/AgCl and 0.4 V *vs.* Ag/AgCl, respectively (Fig. S18). With these potentials, ΔV_{min} values of 0.7 V for C_6-Tri-EDOT and 0.8 V for C_2-EPE were calculated, which are significantly lower than those required for EDOT and ProDOT. Thus, in theory, it is possible to trigger the electropolymerization with lower P_{hv} values (Table S1). In order to test this, the amount of poly-C_6-Tri-EDOT was evaluated as a function of P_{hv} under constant t_{hv} (10 min). Notably, when irradiating the red LED with a P_{hv} of 7×10^{-3} kW cm^{-2}, the potentiodynamic response of poly-C_6-Tri-EDOT, in a monomer-free 0.1 M TBAP/ACN solution, presents two main redox peaks (≈ −0.1 V *vs.* Ag/AgCl and −0.4 V *vs.* Ag/AgCl, respectively) which are associated with the charge/discharge of the film (Fig. 2b). Hence, the use of the trimer unit allows decreasing by three orders of magnitude the P_{hv} required to initiate the electropolymerization, compared with the monomeric units. This was further corroborated by the electropolymerization of C_2-EPE, since under the same experimental conditions, charge/discharge signals around −0.2 V *vs.* Ag/AgCl and −0.5 V *vs.* Ag/AgCl were observed during the potentiodynamic analysis (Fig. S19). Moreover, for both trimers, the magnitude of the main redox signals increases as a function of the applied P_{hv} (Fig. 2b and Fig. S19). These conditions produce light and dark purple films for C_6-tri-EDOT and C_2-EPE, respectively (Fig. 2c).

It is noteworthy that at P_{hv} values above 6×10^{-2} kW cm^{-2}, the ΔV_{hv} is high enough to surpass the oxidation and reduction thresholds of the trimers and Q, respectively. Nonetheless, as it is well-known, when performing the electropolymerization at high potential values (above the oxidation peak), the interface is enriched with highly reactive species (radical cations), which catalyse the oligomerization.[12] This is evidenced by the plot of the Q_a and Q_c as a function of P_{hv} (Fig. 2d). For an energy density of less than 6×10^{-2} kW cm^{-2}, the redox charge of the polymer increases gradually up to 50 μC (Fig. S20). Above this value, Q_a and Q_c increase in a non-linear way by up to one order of magnitude, indicating catalyzed oligomerization (Fig. 2d). In addition, when applying high P_{hv} values (above 2.1 kW cm^{-2}) the potentiodynamic response of both films presents wider peaks and capacitive-like responses at potentials above the main redox process (Fig. 2b and Fig. S19). Thus, under these conditions, the formation of oligomers with a larger range of chain lengths is favored.[12]

Finally, we decided to further simplify this approach by exploring the possible use of a commercial light source from a mobile phone. First, the power density of the lamp and the ΔV_{hv} induced on the red diode were evaluated. Surprisingly, the lamp of the mobile phone produced a P_{hv} of 4.2×10^{-3} kW cm^{-2}, which, when illuminating the diode from a distance of 1 cm, induced a ΔV_{hv} of 0.81 V. According to the potentiodynamic analysis, this is sufficient to trigger the redox reactions.

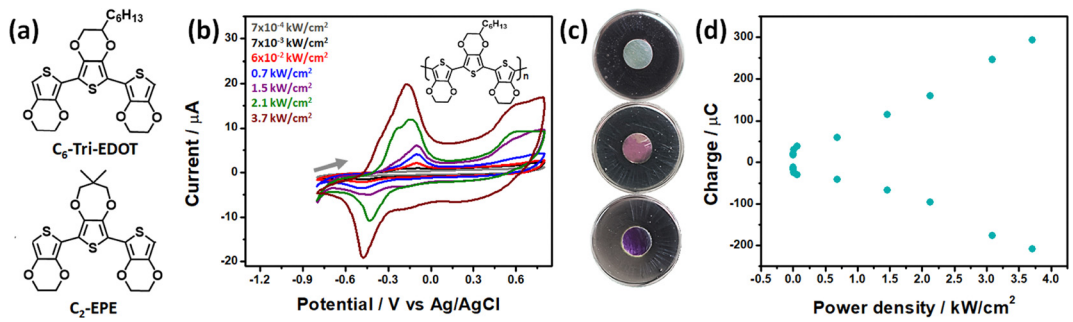

Fig. 2 (a) Chemical structures of C_6-Tri-EDOT and C_2-EPE. (b) Potentiodynamic characterization of poly-C_6-Tri-EDOT films deposited on Pt electrodes as a function of P_{hv} (indicated in the figure) for a constant t_{hv} (10 min), obtained in a monomer-free 0.1 M TBAP/ACN solution, v = 50 mV s^{-1}. (c) Optical pictures of the electrode surface obtained before (top) and after electropolymerization of C_6-Tri-EDOT (middle) and C_2-EPE (bottom) at a constant P_{hv} and t_{hv} (2.1 kW cm^{-2} and 10 min, respectively). (d) Q_a and Q_c variation as a function of P_{hv} used for the light-driven electrocatalytic polymerization of C_6-Tri-EDOT.

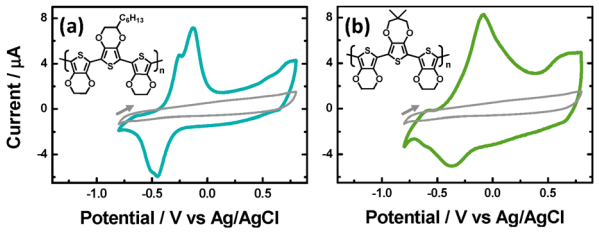

Fig. 3 Potentiodynamic characterization of (a) poly-C_6-Tri-EDOT and (b) poly-C_2-EPE films deposited on Pt electrodes with a constant P_{hv} (4.2×10^{-3} kW cm^{-2}) and t_{hv} (30 min under mobile phone light), obtained in a monomer-free 0.1 M TBAP/ACN solution, v = 50 mV s^{-1}.

Therefore, the light-driven electropolymerization was tested in 0.1 M TBAP/ACN solution containing 10 mM of trimer with a constant t_{hv} (30 min). After this time, the potentiodynamic response of poly-C_6-Tri-EDOT and poly-C_2-EPE, in a monomer-free 0.1 TBAP/ACN solution, exhibits the characteristic irreversible charge/discharge signals with a ΔE_p of 570 mV and 460 mV, respectively (Fig. 3a and b). Moreover, the Q_a and Q_c values (between 70 µC and 110 µC and −50 µC and −84 µC, respectively), measured for both polymers, are comparable to the ones obtained for PEDOT and PProDOT when applying 3-orders of magnitude higher P_{hv} (3.7 kW cm^{-2}) for 20 min. These results demonstrate the possible use of a standard phone light to trigger the electrocatalytic polymerization of π-conjugated trimers.

In conclusion, a novel wireless electropolymerization approach, based on the voltage generating function of a red LED, was developed. The linear correlation between the irradiation time, under constant power density, and the anodic and cathodic charge of PEDOT and PProDOT demonstrates a kinetically controlled polymerization. By fine-tuning the chemical structure of the thiophene, a 3-fold decrease in the power density required to trigger the redox reactions was observed. Moreover, a one order of magnitude increase of the anodic and cathodic charge of the films was obtained during the electrocatalytic polymerization of the 3,4-alkoxythiophene trimers at high power densities. Finally, the smartphone light-driven electrocatalytic polymerization allows the production of films with well-defined redox signals. This proof-of-concept study opens up new interesting alternatives for light-driven wireless synthesis of π-conjugated polymers with a simple experimental setup and low-cost ingredients (Pt electrodes, TBAP/ACN, a monomer, a smartphone and an LED).

Conflicts of interest

There are no conflicts to declare.

Data availability

The data that support the findings of this study are available from the corresponding author upon reasonable request.

Supplementary information (SI): detailed description of the methodology and additional results. See DOI: https://doi.org/10.1039/d5cp03956h.

Acknowledgements

This work has been supported by the French National Research Agency (ANR) in the frame of the project CHIRA-SENSEO (ANR-23-CE42-0004-01).

References

1 (*a*) K. Yan, P. K. Kannan, D. Doonyapisut, K. Wu, C. H. Chung and J. Zhang, *Adv. Funct. Mater.*, 2021, **31**, 2008227; (*b*) B. Zhang, C. Wu, Y. Bao, P. Zou, X. Wang, S. Yuan, G. Chen and C. Chen, *J. Colloid Interface Sci.*, 2025, **677**, 151–160; (*c*) B. Zhang, P. Zou, J. Jiang, S. Yuan, G. Chen and C. Chen, *Chem. Eng.*, 2025, **515**, 163455; (*d*) Y. Xiong, Y. Li, X. Cui, S. Li, X. Peng, Y. Ju, T. Zhou, R. Feng, Y. Zhang, Z. Wang, Q. Wang and L. Dong, *Adv. Funct. Mater.*, 2025, **35**, 2419661; (*e*) D. Liu, C. Huyan, Z. Wang, Z. Guo, X. Zhang, H. Torun, D. Mulvihill, B. B. Xi and F. Chen, *Mater. Horiz.*, 2023, **10**, 2800–2823.

2 (*a*) X. Guo and A. Facchetti, *Nat. Mater.*, 2020, **19**, 922–928; (*b*) B. N. Reddy, M. Deepa and A. G. Joshi, *Phys. Chem. Chem. Phys.*, 2014, **16**, 2062–2071; (*c*) T. Nicolini, A. Villarroel Marquez, B. Goudeau, A. Kuhn and G. Salinas, *J. Phys. Chem. Lett.*, 2021, **12**, 10422–10428; (*d*) T. Soganci, H. C. Soyleyici and M. Ak, *Phys. Chem. Chem. Phys.*, 2016, **18**, 14401–14407; (*e*) I. Bargigia, L. R. Savagian, A. M. Österholm, J. R. Reynolds and C. Silva, *J. Am. Chem. Soc.*, 2021, **143**, 294–308; (*f*) R. Shomura, K. Sugiyasu, T. Yasuda, A. Sato and M. Takeuchi, *Macromolecules*, 2012, **45**, 3759–3771.

3 (*a*) J. Heinze, B. A. Frontana-Uribe and S. Ludwigs, *Chem. Rev.*, 2010, **110**, 4724–4771; (*b*) F. A. Bravo-Plascencia, M. P. Flores-Morales, A. Kuhn, G. Salinas and B. A. Frontana-Uribe, *J. Mater. Chem. A*, 2025, **13**, 27772–27793.

4 (*a*) K. A. Kurdi, S. A. Gregory, M. P. Gordon, J. F. Ponder Jr, A. Atassi, J. M. Rinehart, A. L. Jones, J. J. Urban, J. R. Reynolds, S. Barlow, S. R. Marder and S. K. Yee, *ACS Appl. Mater. Interfaces*, 2022, **14**, 29039–29051; (*b*) P. Sakunpongpitiporn, K. Phasuksom, N. Paradee and A. Sirivat, *RSC Adv.*, 2019, **9**, 6363–6378.

5 (*a*) G. Salinas, A. A. Villegas-Barron, J. Tadeo-Leon and B. A. Frontana-Uribe, *Electrochim. Acta*, 2023, **439**, 141673; (*b*) F. A. Bravo-Plascencia, M. P. Flores-Morales, G. Salinas and B. A. Frontana-Uribe, *Electrochim. Acta*, 2025, **511**, 145375.

6 (*a*) C. B. Tran, T. F. Otero, J. Travas-Sejdic, Q. B. Le and R. Kiefer, *Synth. Met.*, 2023, **299**, 117466; (*b*) H. Yu, A. Marks, S. M. Tuladhar, N. Siemons, I. Anderson, S. Bidinger, S. T. Keene, T. J. Quill, R. Wu, O. Gough, G. Wu, F. Eisner, A. Salleo, J. Rivnay, G. G. Malliaras, P. R. F. Barnes, I. McCulloch and J. Nelson, *Angew. Chem., Int. Ed.*, 2025, **64**, e202417897; (*c*) Q. Guo, Z. Duan, J. Cui, X. Song, Y. Han and J. Liu, *ACS Appl. Polym. Mater.*, 2025, **7**, 12530612539; (*d*) G. Salinas and B. A. Frontana-Uribe, *ChemElectroChem*, 2019, **6**, 4105–4117.

7 (*a*) T. Watanabe, M. Ohira, Y. Koizumi, H. Nishiyama, I. Tomita and S. Inagi, *ACS Macro Lett.*, 2018, **7**, 551–555; (*b*) Y. Zhou, N. Shida, Y. Koizumi, T. Watanabe, H. Nishiyama, I. Tomita and S. Inagi, *J. Mater. Chem. C*, 2019, **7**, 14745.

8 (*a*) Y. Boukarkour, S. Reculusa, N. Sojic, A. Kuhn and G. Salinas, *Chem. – Eur. J.*, 2024, **30**, e202400078; (*b*) G. Salinas, S. Arnaboldi, G. Bonetti, R. Cirilli, T. Benincori and A. Kuhn, *Chirality*, 2021, **33**, 875–882; (*c*) G. Salinas, S. M. Beladi-Mousavi, L. Gerasimova, L. Bouffier and A. Kuhn, *Anal. Chem.*, 2022, **94**, 14317–14321.

9 (*a*) G. T. Cheek, *J. Chem. Educ.*, 2015, **92**, 1049–1052; (*b*) T. Cesin-AbouAtme, C. G. Lopez-Almeida, G. Molina-Labastida and J. G. Ibanez, *J. Chem. Educ.*, 2021, **98**, 3045–3049; (*c*) Y. Zhao, Y. Leger, J. Descamps, N. Sojic and G. Loget, *Small*, 2024, **20**, 2308023.

10 K. Meerholz and J. Heinze, *Electrochim. Acta*, 1996, **41**, 11–12.

11 (*a*) D. Mantione, E. Istif, G. Dufil, L. Vallan, D. Parker, C. Brochon, E. Cloutet, G. Hadziioannou, M. Berggren, E. Stavrinidou and E. Pavlopoulou, *ACS Appl. Electron. Mater.*, 2020, **2**, 4065–4071; (*b*) E. Istif, D. Mantione, L. Vallan, G. Hadziioannou, C. Brochon, E. Cloutet and E. Pavlopoulou, *ACS Appl. Mater. Interfaces*, 2020, **12**, 8695–8703.

12 C. C. B. Bufon, J. Vollmer, T. Heinzel, P. Espindola, H. Hohn and J. Heinze, *J. Phys. Chem. B*, 2005, **109**, 19191–19199.